

1 **Deep Residual Convolutional Neural Network**
2 **Combining Dropout and Transfer Learning for ENSO**
3 **Forecasting**

4 **Jie Hu^{1,2,3*}, Bin Weng^{1,2,3†}, Tianqiang Huang^{1,2,3}, Jianyun Gao⁴, Feng Ye^{1,2,3},**

5 Lijun You⁵

6 ¹College of Mathematics and Informatics, Fujian Normal University, Fuzhou 350007, China

7 ²Digital Fujian Institute of Big Data Security Technology, Fuzhou 350007, China

8 ³Engineering Technology Research Center for Public Service Big Data Mining and Application of Fujian
9 Province, Fuzhou 350007, China

10 ⁴Fujian Key Laboratory of Severe Weather, Fujian Institute of Meteorological Sciences, Fuzhou 350007,
11 China

12 ⁵Fujian Meteorological Information Center, Fuzhou 350007, China

13 **Key Points:**

- 14 • Deep residual convolutional neural network is designed to forecast the amplitude
15 and type of ENSO
- 16 • The prediction skill is improved by applying dropout and transfer learning
- 17 • Our method can successfully predict 20 months in advance for the period between
18 1984 and 2017

*Co-first authors

†Co-first authors

Corresponding author: Tianqiang Huang, fjhtq@fjnu.edu.cn

Corresponding author: Jianyun Gao, fzgaojyun@163.com

19 **Abstract**

20 To improve El Niño-Southern Oscillation (ENSO) amplitude and type forecast, we pro-
 21 pose a model based on a deep residual convolutional neural network with few parame-
 22 ters. We leverage dropout and transfer learning to overcome the challenge of insuffi-
 23 cient data in model training process. By applying the dropout technique, the model effectively
 24 predicts the Niño3.4 Index at a lead time of 20 months during the 1984-2017 evaluation
 25 period, which is three more months than that by the existing optimal model. Moreover,
 26 with homogeneous transfer learning this model precisely predicts the Oceanic Niño In-
 27 dex up to 18 months in advance. Using heterogeneous transfer learning this model achieved
 28 83.3% accuracy for forecasting the 12-month-lead EI Niño type. These results suggest
 29 that our proposed model can enhance the ENSO prediction performance.

30 **Plain Language Summary**

31 El Niño-Southern Oscillation (ENSO) is an irregular periodic variation along with
 32 complex tropical atmosphere-ocean interaction. It impacts interannually human lives glob-
 33 ally and locally. Hence, we contribute, the first time as we know, a deep learning model
 34 that can effectively predict EI Niño strength and type. The model can transfer the knowl-
 35 edge learned from Niño3.4 Index prediction to Oceanic Niño Index and type prediction,
 36 respectively. We find that our proposed model has a high correlation skill and a good
 37 precision for predicting strength and type respectively in relation to an evaluation be-
 38 tween 1984-2017. Moreover, our model requires smaller-sized storage against the exist-
 39 ing deep learning model.

40 **1 Introduction**

41 The EI Niño-Southern Oscillation (ENSO) is one of the main drivers of inter-annual
 42 climate variability on Earth, impacting global climate (Yang et al., 2018), agriculture
 43 (Henson et al., 2017), ecosystems (Lehodey et al., 2020), health (Heaney et al., 2019),
 44 and society (Hsiang et al., 2011). Therefore, it is valuable to predict ENSO early and
 45 accurately to minimize these effects. However, predicting the strength of ENSO remains
 46 a challenge due to its complexity (Timmermann et al., 2018; Sun et al., 2016). Also, the
 47 increasing diversity of ENSO behavior since 2000 has led to a growing interest in the type
 48 of ENSO events (Geng et al., 2020). ENSO can be mainly divided into Eastern Pacific
 49 (EP) and Central Pacific (CP) types (Yeh et al., 2009), based on the distribution of the
 50 Sea Surface Temperature Anomaly (SSTA) during its maturation phase. However, some
 51 events that the SSTA is relatively high over the central and eastern Pacific Ocean can-
 52 not be classified as CP or EP types. Zhang et al. (2019) classified ENSO into EP, CP,
 53 and a mixture of the two (MIX) types of EI Niño (La Niña). To the best of our knowl-
 54 edge, the definition of ENSO type has not come to an agreement. Because the effects
 55 of different ENSO types vary greatly, e.g., different EI Niño events have a different im-
 56 pact on US winter temperatures (Yu et al., 2012) and the East Asian climate (Yuan &
 57 Yang, 2012). Hence, the prediction of ENSO type is important for improving the qual-
 58 ity of climate forecasts.

59 Currently, both statistical (Petrova et al., 2020; Ren, Zuo, & Deng, 2018; Wang et
 60 al., 2020) and dynamical (Saha et al., 2014; Ren, Scaife, et al., 2018) methods can gen-
 61 erate skillful predictions 6-12 months in advance. Many deep learning-based methods
 62 have emerged in recent years, e.g. using Artificial Neural Networks (ANNs) (Petersik &
 63 Dijkstra, 2020; Feng et al., 2016), Recurrent Neural Networks (RNNs) (Mahesh et al.,
 64 2019), Long Short-Term Memory (LSTM) neural networks (Broni-Bedaiko et al., 2019),
 65 Convolutional Long Short-Term Memory (ConvLSTM) (Mu et al., 2019; Gupta et al.,
 66 2020; D. He et al., 2019), Convolutional Neural Networks (CNNs) (Ham et al., 2019; Yan
 67 et al., 2020), and Graph Neural Networks (GNNs) (Cachay et al., 2020). The most re-
 68 markable work is the CNN-based model that can make effective forecasts 17 months in

advance (Ham et al., 2019), outperforming most existing methods. This model is trained on Coupled Model Intercomparison Project phase5 (CMIP5) and reanalysis data to predict the Niño3.4 index. However, the model has few layers, only convolutional and pooling layers, does not use residual structures, and does not use some techniques to improve the predictability except for the use of transfer learning on CMIP5. Recent studies have shown that the dropout technology can improve the performance of shallow neural networks applied to temperature simulation problems (Piotrowski et al., 2020). Through extensive experiments they show that improving model performance and stability requires nodes to be discarded with much lower probability than common deep neural networks (about 1%, instead of 10-50% for deep learning). Due to a number of layers applied in our model, we consider using the dropout in more detail to further improve the prediction ability. Additionally, comparing to the existing research on ENSO prediction which only performs transfer learning on simulated data, we also consider transferring the knowledge learned from the task of predicting the Niño3.4 index to the tasks of predicting Oceanic Niño Index (ONI), so-called homogeneous transfer learning.

There are various methods of predicting ENSO types, e.g. based on the random forest (Santos et al., 2020), multi-model ensemble (Ren, Scaife, et al., 2018), and CNN (Ham et al., 2019). In this work, we focus on the CNN method trained on CMIP5 data to predict El Niño types. The accuracy remains 66.7% at lead times of 12 months. However, they have only expected the types of El Niño, not yet the types of La Niña and the normal events. Besides, using transfer learning in the index prediction leads to a slight performance improvement, while in the type prediction, no transfer learning is used. Nevertheless, we can transfer the knowledge learned from the task of index prediction to type prediction. This method is called heterogeneous transfer learning, thereby further improving the prediction ability.

In this work, the main contributions are summarized as follows:

1. We propose a deep Residual Convolutional Neural Network (Res-CNN) model for ENSO predictions, including the Niño3.4 index, ONI, and types. It is worth noting that our model requires only a few changes for different tasks. We find that the Res-CNN model can effectively predict the Niño3.4 index for up to 20 months in advance, three months more than the previous CNN-based model.
2. Keeping the network structure intact, we show the ONI can be skillfully predicted 18 (12) months in advance with (without) homogeneous transfer learning, which provides us a new strategy for further enhancing the predictive ability of ENSO.
3. We apply heterogeneous transfer learning to enhance the type prediction. We show that the knowledge learned from the index prediction task can be transferred to the type prediction task by changing only the output layer of the model trained for the index prediction task and retraining on the type prediction task. The accuracy of El Niño type prediction can reach 83.3% 12 months in advance, while the current best is 66.7%.

2 Data and Methods

2.1 Data

The predictors are three consecutive months SSTA and Heat Content Anomaly (vertically averaged oceanic temperature anomaly in the upper 300 m) over 0°-360°E, 55°S-60°N at a resolution of 5°×5°. The simulated dataset is CMIP5 3.2 (core) (1861-2004) (Bellenger et al., 2014). The reanalysis dataset is simple ocean data assimilation version 2.2.4 (SODA) (1871-1973) (Giese & Ray, 2011) and Global Ocean Data Assimilation System (GODAS) (1982-2017) (Behringer & Xue, 2004).

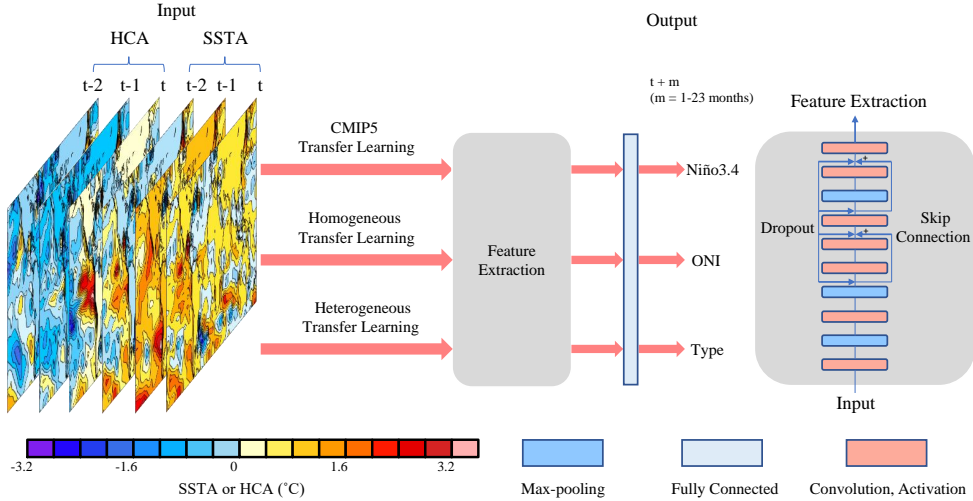


Figure 1. The architecture of the Res-CNN model. The variables of the input layer correspond to the sea surface temperature (in units of $^{\circ}\text{C}$) anomaly and the oceanic heat content (in units of $^{\circ}\text{C}$) anomaly from time $t - 2$ months to t months, between 0° – 360°E and 55°S – 60°N . The three-month-averaged Niño3.4 index, ONI and ENSO type from time $t + 1$ months to $t + 23$ months is used as a variable for the output layer.

117

2.2 Res-CNN model

The input data for three consecutive months are recorded as x_{t-2}, x_{t-1}, x_t , the output data of the Niño3.4 index, ONI or type all referred to as y , and the forecast result can be described by

$$y_{t+l} = F_l(x_{t-2}, x_{t-1}, x_t) \quad (1)$$

where F denotes the Res-CNN model, and l is the forecast lead months from 1 to 23. Res-CNN shown in Figure 1 uses a 7-layer convolutional neural network, a 3-layer max-pooling to extract features, 2-layer skip connections, and 1-layer fully connected layer to generate the final result. In index predicting task, the output is a single value; while in type predicting task, the output is the probability of various categories. The convolution process of Res-CNN is the most efficient computational tool for extracting features as follows:

$$v_{l,f}^{x,y} = \sum_{m=1}^{M_{l-1}} \sum_{p=1}^{P_l} \sum_{q=1}^{Q_l} w_{l,f,m}^{p,q} v_{(l-1),m}^{(x+p-P_l/2, y+q-Q_l/2)} + b_{l,f} \quad (2)$$

118
119
120
121
122

Where (x, y) is the dimensions of the feature map, l denotes the l -th convolution layer, and f is for the f -th feature map. M means the number of feature maps, and (P_l, Q_l) is the dimensions of the l -th filter. b is the bias units, w is the weight at grid point (p, q) in the convolution kernel and $v_{l,f}$ denotes one value of the l -th filter and the f -th feature map.

The parameters of our model are learned through multiple iterations of the minimization loss function of Mean Square Error in predicting index or Cross Entropy in predicting type. In our model, the residual structure can be defined as follows

$$y = R(x, \{W\}) + x \quad (3)$$

123 where x and y are the input and output vectors of the considered layer, and the function R denotes the residual mapping to be learned. The operation $R+x$ is performed
 124 by a shortcut connection and element-wise addition. The other details are same as those
 125 in K. He et al. (2016), except that we use the Tanh activation function instead of the
 126 rectified linear unit and do not use the batch normalization (Ioffe & Szegedy, 2015). Be-
 127 cause our network is shallow compared to a standard residual network, small changes
 128 in network parameters have little effect when the network is not deep. Also, because our
 129 data is insufficient and complex, if the input of each layer of the network is kept the same
 130 distribution, the model cannot be trained well. Setting the number of residual connec-
 131 tions to 0, 1, 2, and 3, our model has various structures. In order to further improve per-
 132 formance, 11 different dropout rates are token, namely 0, 0.01, 0.03, 0.05, 0.07, 0.1, 0.3,
 133 0.5, 0.7, 0.9, 0.99. Thus, for each advance month, there are 44 models (Figure S1). The
 134 final model would be the best result from the model that determines the number of resid-
 135 ual connections. See Text S1 for details on dropout and transfer learning techniques.
 136

137 2.3 Indexes forecast

In predicting index includes the Niño3.4 index and ONI. The number of the unit
 138 in fully connected layer is one, and the Adam (Kingma & Ba, 2014) optimization algo-
 139 rithm is used. The specific parameter settings can be found in the Text S2. We use the
 140 correlation coefficient function I as a measure of the ENSO index prediction:
 141

$$I_l = \sum_{t=1}^{12} \frac{\sum_{y=s}^e (O_{y,t} - \bar{O}_t) (F_{y,t,l} - \bar{F}_{t,l})}{\sqrt{\sum_{y=s}^e (O_{y,t} - \bar{O}_m)^2 \sum_{y=s}^e (F_{y,t,l} - \bar{F}_{t,l})^2}} \quad (4)$$

138 where, O and F denote the observed and the predicted values, respectively. $\bar{O}_{t,l}$ and $\bar{F}_{t,l}$
 139 denote the temporal climatology concerning the calendar month m (from 1 to 12) and
 140 the forecast lead months l (from 1 to 23). The label y means the forecast target year.
 141 Finally, s and e denote the earliest and latest validation or test year.

142 2.4 Types forecast

We conduct two kinds of experiments: one is to predict three types, i.e. EP, CP,
 143 and MIX of EI Niño; and the other is with seven types, i.e. EP, CP, MIX of EI Niño (La
 144 Niña), and Normal Year (NY). See the Text S3 for more details.
 145

146 3 Results

The All-season Correlation Skill (ACS) is shown in Figure 2 for the CNN (b) and
 147 the Res-CNN (c). The ACS of the three-month-moving-averaged Niño3.4 index between
 148 1984 and 2017 in the Res-CNN model is higher than almost all state-of-the-art dynamic
 149 models and the CNN model (Figure 2a). It is worth noting that, except for the Res-CNN
 150 model, the CNN model fails to perform optimally when the lead time is less than 6 months.
 151 The correlation coefficient of the CNN model exceeds 0.5 only 17 months in advance, and
 152 worse than the Scale Interaction Experiment-Frontier (SINTEX-F) dynamic prediction
 153 model [40] for a lead of 23 months, while the Res-CNN model reaches 20 months in ad-
 154 vance and outperforms the SINTEX-F dynamic prediction model in all advance months.
 155 Thus, we conclude that the Res-CNN model can skillfully predict ENSO 20 months in
 156 advance, which is better than all the compared models. The Res-CNN model exhibits
 157 a higher correlation coefficient than the CNN model in almost all target seasons, espe-
 158 cially in spring and autumn seasons. For example, when the target season is MJJ (May-
 159 June-July), the SINTEX-F model predicts a correlation coefficient above 0.5 for only four
 160 months (Table S3), the CNN model for 11 months (Figure 2b), and the Res-CNN model
 161 for 17 months (Figure 2c), suggesting that our model is less affected by the spring pre-
 162 diction barrier (SPB) than the CNN and SINTEX-F model. Typically, the SPB phenomenon
 163

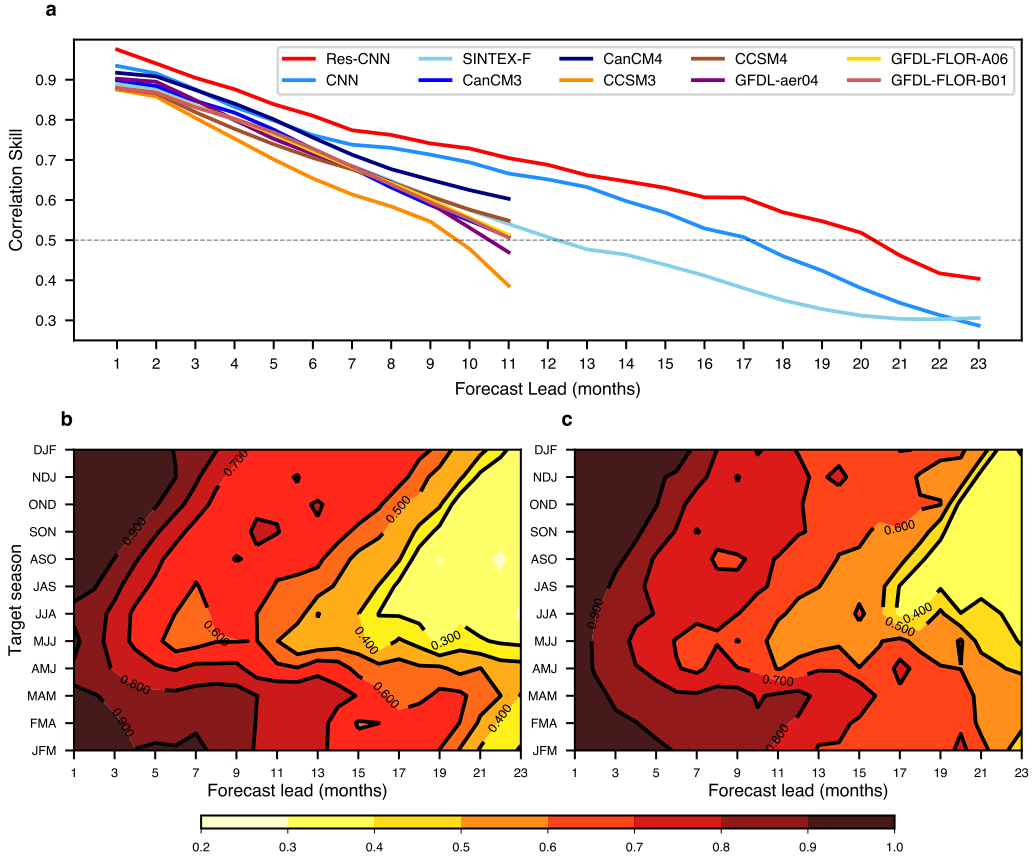


Figure 2. Correlation skill for various lead times and methods. All season correlation skill of the three-month-moving-averaged Niño3.4 index for multiple lead times from 1984 to 2017 in the Res-CNN model (red), CNN model (Ham et al., 2019) (dodger blue), SINTEX-F (Luo et al., 2008) dynamical forecast system (sky blue), and other dynamical forecast systems (Kirtman et al., 2014) included in the North American Multi-Model Ensemble (NMME) project (the other colors). The correlation skill of the Niño3.4 index for each season in the CNN model (b) and the Res-CNN model (c). The black dashed line indicates that the correlation coefficient is equal to 0.5.

164 is more severe in statistical models than in dynamic models (Jan van Oldenborgh et al.,
 165 2005). The Res-CNN model is less affected than other statistical methods because it is
 166 likely to make fuller use of the heat content information than other statistical methods,
 167 and accurate initialization of heat content can improve spring forecasting (McPhaden,
 168 2003). Nevertheless, the skills are much lower for summer time than winter, which may
 169 be related to the predictability. And the "spring barrier" (western pacific ocean) may
 170 be a main factor to impact the summer predictability.

171 The ACS of the three-month-moving-averaged Niño3.4 index from 1982 to 2001 and
 172 from 2002 to 2017 is shown in Figure S2. Whether it is 82-01 or 02-17, the prediction
 173 skill in the Res-CNN model is higher than the CNN model in all months ahead. How-
 174 ever, compared with the skill between 1982 and 2001, 2002-2017 declines sharply, with
 175 its effective prediction only 12 months. Similarly, the CNN model drops to only ten months,
 176 which is inseparable because the behavior of ENSO becomes more diverse after 2000 (Barnston
 177 et al., 2012). To assess the effect of the actual prediction more clearly in the Res-CNN
 178 model, we generated curves of the Niño3.4 index predicting the DJF season 18 months
 179 in advance for the years 1982 to 2017 (Figure S3). Compared to the SINTEX-F model,
 180 the Res-CNN correlation coefficient is over 0.2 higher. Besides, the Res-CNN also has
 181 correlation coefficient of 0.2 higher than the CNN model 20 months in advance (Figure
 182 S4), better predicting years with higher Niño3.4 index, such as 1982/1983, 1997/1998.

183 The ACS of the ONI is shown in Figure 3 for the Gaussian Density Neural Net-
 184 work (GDNN) (a), the Quantile Regression Neural Network (QRNN) (b), and the Res-
 185 CNN (c). Compared to the GDNN and QRNN methods (Petersik & Dijkstra, 2020), the
 186 ACS of the ONI between 1984 and 2017 in the Res-CNN model using homogeneous trans-
 187 fer learning is highest (Figure 3d). Notably, the correlation coefficients of GDNN and
 188 QRNN in predicting ONI from 2002 to 2011 drop below 0.5 at 7 months ahead, while
 189 our method still has 0.6 at 10 months ahead, which is almost consistent with Niño 3.4
 190 in predicting 2002 to 2017. Besides, comparing the results of predicting Niño3.4 index
 191 and ONI from 1982 to 2017, ONI gives better results until the advance month is 12, while
 192 Niño3.4 index gives better results after that, suggesting that for index prediction with
 193 greater than one year, the amount of data has an impact on the model.

194 The results of 3, 6, 9, 12, 18, 23 months ahead forecasts of El Niño types from 1982
 195 to 2017 are shown in Table 1. We found that compared to using one-step, using two-step
 196 achieves better results in all five scenarios of A-E; comparing A-two with B-two and C-
 197 two with E-two, the results of A are not as good as those of B and C's are not as good
 198 as E's. This indicates that the pre-training and soda training methods are not as good
 199 as just using the pre-training method in type prediction, in the meantime, the distribu-
 200 tion of SODA and GODAS data is very inconsistent, possibly due to the significant dif-
 201 ference in the frequency of occurrence of various types in the SODA dataset (Yeh et al.,
 202 2009) and the diversity after 2000 (Barnston et al., 2012). Compared with A-two and
 203 C-two, our model can still achieve 67% accuracy under 12 months ahead using hetero-
 204 geneous transfer learning. Also, it can predict all super ENSO 12 months in advance,
 205 especially the 2015/2016 EI Niño, the strongest events in history, which can still be pre-
 206 dicted at a lead time of 18 months. At present, almost all models cannot predict the event
 207 one year in advance (Tang et al., 2018). By comparing the results of A-two and D-two,
 208 the accuracy of A-two is lower than that of D-two, indicating that transfer training on
 209 SODA instead reduces the accuracy of most of the models initially trained on CMIP5.
 210 This suggests that fine-tuning on SODA does not yield better results, probably because
 211 heterogeneous transfer learning has been able to resolve, to some extent, the problem
 212 of unbalanced data distribution between CMIP5 and SODA.

213 Finally, to evaluate the performance of our model, we compare it with the CNN
 214 model. Figure S5 shows our model achieves 83.3% accuracy 12 months earlier on the pe-
 215 riod from 1984 to 2017 compared to the CNN model (66.7% accuracy). These results

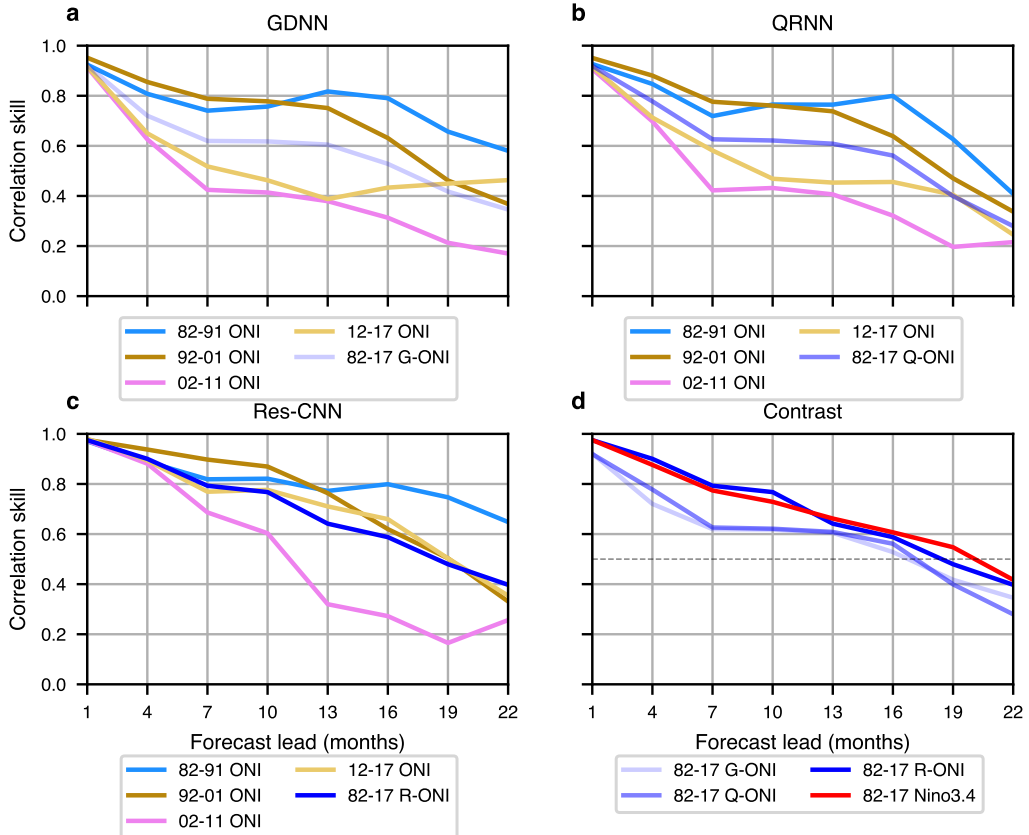


Figure 3. Correlation skill of the ONI for various lead times, decades, and models. The all-season correlation skill of the ONI from 1982 to 1991, from 1992 to 2001, from 2002 to 2011, from 2012 to 2017, from 1982 to 2017 using GDNN (a), QRNN (b) and Res-CNN (c) with transfer learning for various lead times. (d) The all-season correlation skill of the ONI between 1982 and 2017 using GDNN, QRNN, and Res-CNN at various lead times, Niño3.4 index using Res-CNN (red). The black dashed line indicates that the correlation coefficient is equal to 0.5.

Table 1. Prediction of ENSO types

Methods	Lead months				
	3	6	9	12	18
A-one	27	22	21	19	14
A-two	32	26	22	22	17
B-one	25	20	17	15	13
B-two	30	24	18	18	16
C-one	29	22	19	19	15
C-two	32	27	24	24	20
D-one	28	23	18	18	16
D-two	29	26	24	21	17
E-one	26	24	16	14	13
E-two	28	26	19	17	17
Super ENSO	3/3	2/3	2/3	2/3	2/2
Accuracy (%)	89/89	72/75	61/67	61/67	47/56

Results of forecasting the types of ENSO 3, 6, 9, 12, 18 months in advance from 1982 to 2017. There are 36 events in total, A-E in the table represents the number of correct predictions. H and N denote the use and non-use of heterogeneous transfer learning, respectively. one means one-step seven classes prediction, two means two-step seven classes prediction, that first predicts El Niño, La Niña, and normal year events, and then predicts whether El Niño or La Niña will be EP, CP, or MIX. Super ENSO means that A-two/C-two correctly predicted the number of 1982/1983, 1997/1998, 2015/2016 EI Niño.

Accuracy indicates that the accuracy of A-two/C-two.

A: Train in CMIP5. B: Train in CMIP5 and then train in SODA.

C: Heterogeneous transfer learning the index model to CMIP5.

D: Homogeneous transfer learning the C to SODA.

E: Heterogeneous transfer learning the index model to CMIP5 and then training in SODA. The model of using heterogeneous transfer is the optimal model for predicting the respective lead and target of the Niño3.4 index.

216 indicate that the Res-CNN model predicts the ENSO index and type better than the CNN
 217 model.

218 4 Discussions

219 Through various dropout experiments, we found that we got better and more sta-
 220 ble results at a lower dropout rate (0-0.3) than those at a higher dropout rate (0.5-0.9)
 221 (Figure S6). The finding differs from the conventional deep learning approach usually
 222 set with 0.4-0.6 of the dropout rate. The achievement is due to fewer parameters of the
 223 network. Therefore, too large dropout rate will lead to significant reduction of the learn-
 224 able parameters of the network during each round of iterations. Hence such training pro-
 225 cess would not produce suitable results. To find the appropriate number of residual con-
 226 nections, we conducted ablation experiments. The obtained results (Figure S7) show that
 227 the effective prediction months were about 17, 18, 20, and 16 when the number of resid-
 228 ual connections was 0, 1, 2, and 3, respectively. It was selected as our optimal model since
 229 the model with residual connections of 2 predicted best. Furthermore, Figure S8 shows
 230 that using un-normalized 2 residual connections achieved significantly better prediction
 231 results in comparison to using normalization, indicating that data normalization does
 232 not improve the model performance in deep learning-based ENSO prediction. Addition-
 233 ally, the model with a residual number of 3 can only predict the effective forecast for 17
 234 months, indicating no further improvement of a higher residual connection number.

235 5 Conclusions

236 Although this study showed remarkable results, there are still some limitations. In
 237 predicting the Niño3.4 index, the predictive ability of Res-CNN is notably improved in
 238 all seasons. However, by comparing the correlation coefficient for lead months from 1 to
 239 23 months, we found that they were nearly the lowest from late spring to fall (Table S1),
 240 the same as CNN (Table S2) and SINTEX-F (Table S3). This suggested that the SPB
 241 is still prevalent (Levine & McPhaden, 2015) and requires further study. Moreover, there
 242 is a large negative anomaly of the predicted SST for the first 10 years for both CNN and
 243 our model, whether this implies a change in climate or for other reasons we also need
 244 to investigate further. Holding the model structure constant to predict ONI, surprisingly,
 245 Res-CNN can effectively predict for 12 months (Figure S9) despite using only a small
 246 amount of data. However, the correlation coefficients were unstable at times high and
 247 low under different months of advance, and did not show a stable downward trend. To
 248 alleviate the problem, we predicted ONI using homogeneous transfer learning, and the
 249 skill was significantly enhanced. Since our model initially predicted the Niño3.4 index
 250 well, we assume that our model could learn to predict it. The ONI definition is closer
 251 to the Niño3.4 index, so the model is able to learn lots of knowledge and only needs less
 252 training to predict the ONI well. By varying only the number of the unit in the output
 253 layer of our model to predict the EI Niño type, the result in Table 1 is still almost 20
 254 percentage points higher than the CNN. Moreover, two-step and heterogeneous trans-
 255 fer learning were used in this work to predict ENSO types, with some predictive perfor-
 256 mance improvement.

257 In summary, this study showed that the Res-CNN-based model can improve the
 258 long-term prediction of ENSO. Also, we found that the predictive ability can be better
 259 improved by using transfer learning and dropout techniques. The future extensions would
 260 be using different numbers of predictors and input months under different prediction months,
 261 e.g., intuitively, trying fewer predictors and input months under shorter advance months.

262 **Acknowledgments**

263 This study was supported by National Key R&D Program Special Fund Grant (No. 2018YFC1505805),
 264 National Natural Science Foundation of China (No. 62072106, No. 61070062), General
 265 Project of Natural Science Foundation in Fujian Province (No. 2020J01168), Open project
 266 of Fujian Key Laboratory of Severe Weather (No. 2020KFKT04). The research data can
 267 be found in (<https://doi.org/10.5281/zenodo.4646653>), and the code used in this
 268 paper are available at this site (<https://github.com/icodeworld/Deep-learning-ENSO>).

269 **References**

- 270 Barnston, A. G., Tippett, M. K., L'Heureux, M. L., Li, S., & DeWitt, D. G. (2012).
 271 Skill of real-time seasonal enso model predictions during 2002–11: Is our ca-
 272 pability increasing? [Journal Article]. *Bulletin of the American Meteorological Society*, 93(5), 631–651. doi: 10.1175/bams-d-11-00111.1
- 273 Behringer, D., & Xue, Y. (2004). Evaluation of the global ocean data assimilation
 274 system at ncep: The pacific ocean. In *Proc. eighth symp. on integrated observ-
 275 ing and assimilation systems for atmosphere, oceans, and land surface*.
- 276 Bellenger, H., Guilyardi, É., Leloup, J., Lengaigne, M., & Vialard, J. (2014). Enso
 277 representation in climate models: From cmip3 to cmip5. *Climate Dynamics*,
 278 42(7), 1999–2018. doi: 10.1007/s00382-013-1783-z
- 279 Broni-Bedaiko, C., Katsriku, F. A., Unemi, T., Atsumi, M., Abdulai, J.-D., Shi-
 280 nomiya, N., & Owusu, E. (2019). El niño-southern oscillation forecasting
 281 using complex networks analysis of lstm neural networks. *Artificial Life and
 282 Robotics*, 24(4), 445–451. doi: 10.1007/s10015-019-00540-2
- 283 Cachay, S. R., Erickson, E., Bucker, A. F. C., Pokropek, E., Potosnak, W., Osei,
 284 S., & Lütjens, B. (2020). Graph neural networks for improved el niño no
 285 forecasting. *arXiv preprint arXiv:2012.01598*.
- 286 Feng, Q. Y., Vasile, R., Segond, M., Gozolchiani, A., Wang, Y., Havlin, S., ... Di-
 287 jkstra, H. A. (2016). Climatelearn: A machine-learning approach for cli-
 288 mate prediction using network measures [Journal Article]. . CC, 18. doi:
 289 10.5194/gmd-2015-273
- 290 Geng, T., Cai, W., & Wu, L. (2020). Two types of enso varying in tandem facil-
 291 itated by nonlinear atmospheric convection [Journal Article]. *Geophysical Re-
 292 search Letters*, e2020GL088784. doi: 10.1029/2020gl088784
- 293 Giese, B. S., & Ray, S. (2011). El niño variability in simple ocean data assimilation
 294 (soda), 1871–2008. *Journal of Geophysical Research: Oceans*, 116(C2). doi: 10
 295 .1029/2010jc006695
- 296 Gupta, M., Kodamana, H., & Sandeep, S. (2020). Prediction of enso beyond spring
 297 predictability barrier using deep convolutional lstm networks. *IEEE Geoscience
 298 and Remote Sensing Letters*. doi: LGRS.2020.3032353
- 299 Ham, Y. G., Kim, J. H., & Luo, J. J. (2019). Deep learning for multi-year enso fore-
 300 casts [Journal Article]. *Nature*, 573(7775), 568–572. Retrieved from <https://www.ncbi.nlm.nih.gov/pubmed/31534218> doi: 10.1038/s41586-019-1559-7
- 301 He, D., Lin, P., Liu, H., Ding, L., & Jiang, J. (2019). Dlenso: A deep learning enso
 302 forecasting model. In *Pacific rim international conference on artificial intelli-
 303 gence* (pp. 12–23). doi: 10.1007/978-3-030-29911-8_2
- 304 He, K., Zhang, X., Ren, S., & Sun, J. (2016). Deep residual learning for image
 305 recognition [Conference Proceedings]. In *2016 ieee conference on computer vi-
 306 sion and pattern recognition (cvpr)* (p. 770–778). Las Vegas, NV, USA: IEEE.
 307 doi: 10.1109/CVPR.2016.90
- 308 Heaney, A. K., Shaman, J., & Alexander, K. A. (2019). El niño-southern oscillation
 309 and under-5 diarrhea in botswana. *Nature communications*, 10(1), 1–9. doi: 10
 310 .1038/s41467-019-13584-6
- 311 Henson, C., Market, P., Lupo, A., & Guinan, P. (2017). Enso and pdo-related
 312 climate variability impacts on midwestern united states crop yields [Jour-
 313

- 315 *nal Article]. International journal of biometeorology*, 61(5), 857-867. doi:
316 10.1007/s00484-016-1263-3

317 Hsiang, S. M., Meng, K. C., & Cane, M. A. (2011). Civil conflicts are associated
318 with the global climate [Journal Article]. *Nature*, 476(7361), 438-441. doi: 10.
319 .1038/nature10311

320 Ioffe, S., & Szegedy, C. (2015). Batch normalization: Accelerating deep network
321 training by reducing internal covariate shift. In *International conference on
322 machine learning* (pp. 448–456).

323 Jan van Oldenborgh, G., Balmaseda, M. A., Ferranti, L., Stockdale, T. N., &
324 Anderson, D. L. T. (2005). Did the ecmwf seasonal forecast model out-
325 perform statistical enso forecast models over the last 15 years? [Jour-
326 nal Article]. *Journal of Climate*, 18(16), 3240-3249. Retrieved from
327 <GotoISI>://WOS:000232051600011 doi: 10.1175/jcli3420.1

328 Kingma, D. P., & Ba, J. (2014). Adam: A method for stochastic optimization. *arXiv
329 preprint arXiv:1412.6980*.

330 Kirtman, B. P., Min, D., Infantti, J. M., Kinter, J. L., Paolino, D. A., Zhang, Q., ...
331 others (2014). The north american multimodel ensemble: phase-1 seasonal-
332 to-interannual prediction; phase-2 toward developing intraseasonal predic-
333 tion. *Bulletin of the American Meteorological Society*, 95(4), 585–601. doi:
334 10.1175/bams-d-12-00050.1

335 Lehodey, P., Bertrand, A., Hobday, A. J., Kiyofuji, H., McClatchie, S., Menkès,
336 C. E., ... Tommasi, D. (2020). Enso impact on marine fisheries and ecosys-
337 tems [Journal Article]. *El Niño Southern Oscillation in a Changing Climate*,
338 429-451. doi: 10.1002/9781119548164.ch19

339 Levine, A. F., & McPhaden, M. J. (2015). The annual cycle in enso growth rate as a
340 cause of the spring predictability barrier. *Geophysical Research Letters*, 42(12),
341 5034–5041. doi: 10.1002/2015GL064309

342 Luo, J.-J., Masson, S., Behera, S. K., & Yamagata, T. (2008). Extended enso predic-
343 tions using a fully coupled ocean–atmosphere model [Journal Article]. *Journal
344 of Climate*, 21(1), 84-93. doi: 10.1175/2007jcli1412.1

345 Mahesh, A., Evans, M., Jain, G., Castillo, M., Lima, A., Lunghino, B., ... others
346 (2019). Forecasting el niño with convolutional and recurrent neural networks.
347 In *33rd conference on neural information processing systems (neurips 2019),
348 vancouver, canada* (pp. 8–14).

349 McPhaden, M. J. (2003). Tropical pacific ocean heat content variations and
350 enso persistence barriers [Journal Article]. *Geophysical Research Let-
351 ters*, 30(9). Retrieved from <GotoISI>://WOS:000182873800003 doi:
352 10.1029/2003gl016872

353 Mu, B., Peng, C., Yuan, S., & Chen, L. (2019). Enso forecasting over multiple
354 time horizons using convlstm network and rolling mechanism [Conference Pro-
355 ceedings]. In *2019 international joint conference on neural networks (ijcnn)*
356 (p. 1-8). Budapest, Hungary: IEEE. doi: 10.1109/IJCNN.2019.8851967

357 Petersik, P. J., & Dijkstra, H. A. (2020). Probabilistic forecasting of el niño using
358 neural network models [Journal Article]. *Geophysical Research Letters*, 47(6),
359 e2019GL086423. doi: 10.1029/2019GL086423

360 Petrova, D., Ballester, J., Koopman, S. J., & Rodó, X. (2020). Multiyear statistical
361 prediction of enso enhanced by the tropical pacific observing system [Journal
362 Article]. *Journal of Climate*, 33(1), 163-174. doi: 10.1175/jcli-d-18-0877.1

363 Piotrowski, A. P., Napiorkowski, J. J., & Piotrowska, A. E. (2020). Impact
364 of deep learning-based dropout on shallow neural networks applied to
365 stream temperature modelling. *Earth-Science Reviews*, 201, 103076. doi:
366 10.1016/j.earscirev.2019.103076

367 Ren, H.-L., Scaife, A. A., Dunstone, N., Tian, B., Liu, Y., Ineson, S., ... MacLach-
368 lan, C. (2018). Seasonal predictability of winter enso types in operational
369 dynamical model predictions [Journal Article]. *Climate Dynamics*, 52(7-8),

- 370 3869–3890. doi: 10.1007/s00382-018-4366-1
- 371 Ren, H.-L., Zuo, J., & Deng, Y. (2018). Statistical predictability of niño indices for
372 two types of enso [Journal Article]. *Climate Dynamics*, 52(9-10), 5361–5382.
373 doi: 10.1007/s00382-018-4453-3
- 374 Saha, S., Moorthi, S., Wu, X., Wang, J., Nadiga, S., Tripp, P., ... others (2014).
375 The ncep climate forecast system version 2. *Journal of climate*, 27(6), 2185–
376 2208.
- 377 Santos, M. A. D. C., Vega-Oliveros, D. A., Zhao, L., & Berton, L. (2020). Clas-
378 sifying el niño-southern oscillation combining network science and ma-
379 chine learning [Journal Article]. *IEEE Access*, 8, 55711–55723. doi:
380 10.1109/access.2020.2982035
- 381 Sun, Y., Wang, F., & Sun, D.-Z. (2016). Weak enso asymmetry due to weak non-
382 linear air-sea interaction in cmip5 climate models [Journal Article]. *Advances*
383 in Atmospheric Sciences, 33(3), 352-364. Retrieved from <GotoISI>://WOS:
384 000370030300008 doi: 10.1007/s00376-015-5018-6
- 385 Tang, Y., Zhang, R.-H., Liu, T., Duan, W., Yang, D., Zheng, F., ... others (2018).
386 Progress in enso prediction and predictability study. *National Science Review*,
387 5(6), 826–839. doi: 10.1093/nsr/nwy105
- 388 Timmermann, A., An, S. I., Kug, J. S., Jin, F. F., Cai, W., Capotondi, A., ...
389 Zhang, X. (2018). El niño-southern oscillation complexity [Journal Arti-
390 cle]. *Nature*, 559(7715), 535-545. Retrieved from <https://www.nature.com/articles/s41586-018-0252-6> doi: 10.1038/s41586-018-0252-6
- 392 Wang, X., Slawinska, J., & Giannakis, D. (2020). Extended-range statistical enso
393 prediction through operator-theoretic techniques for nonlinear dynamics. *Sci-
394 entific reports*, 10(1), 1–15. doi: 10.1038/s41598-020-59128-7
- 395 Yan, J., Mu, L., Wang, L., Ranjan, R., & Zomaya, A. Y. (2020). Temporal convolu-
396 tional networks for the advance prediction of enso. *Scientific reports*, 10(1), 1–
397 15. doi: 10.1038/s41598-020-65070-5
- 398 Yang, S., Li, Z., Yu, J.-Y., Hu, X., Dong, W., & He, S. (2018). El niño-southern os-
399 cillation and its impact in the changing climate [Journal Article]. *National Sci-
400 ence Review*, 5(6), 840-857. doi: 10.1093/nsr/nwy046
- 401 Yeh, S. W., Kug, J. S., Dewitte, B., Kwon, M. H., Kirtman, B. P., & Jin, F. F.
402 (2009). El nino in a changing climate [Journal Article]. *Nature*, 461(7263),
403 511-4. doi: 10.1038/nature08316
- 404 Yu, J., Zou, Y., Kim, S. T., & Lee, T. (2012). The changing impact of el niño on
405 us winter temperatures [Journal Article]. *Geophysical Research Letters*, 39(15).
406 doi: 10.1029/2012gl052483
- 407 Yuan, Y., & Yang, S. (2012). Impacts of different types of el niño on the east asian
408 climate: Focus on enso cycles [Journal Article]. *Journal of Climate*, 25(21),
409 7702-7722. doi: 10.1175/jcli-d-11-00576.1
- 410 Zhang, Z., Ren, B., & Zheng, J. (2019). A unified complex index to characterize two
411 types of enso simultaneously [Journal Article]. *Scientific reports*, 9(1), 1-8. doi:
412 10.1038/s41598-019-44617-1